Title
Detecting stable phase structures in EEG signals to classify brain activity amplitude patterns

Journal
Journal of Zhejiang University - Science A, 10(10)

Authors
Ruiz, Yusely
Li, Guang
Freeman, Walter J, III
et al.

Publication Date
2009-10-01

DOI
10.1631/jzus.A0820690

Peer reviewed

Detecting stable phase structures in EEG signals to classify brain activity amplitude patterns

First Author: Yusely Ruiz,
First Author's Institution: Biomedical Engineering Department, Zhejiang University, China.
Email:yuselyrg79@yahoo.es

Corresponding Author: Guang Li
Corresponding Author's Institution: National Laboratory of Industrial Control Technology, Institute of Cyber-Systems and Control, Zhejiang University, Hangzhou, 310027, China
Email: guangli@zju.edu.cn

Other Author: Walter J. Freeman
Other Author's Institution: Department of Molecular & Cell Biology, 101 Donner University of California at Berkeley, CA 94720-3206 USA.
Email: dfreeman@berkeley.edu

Other Author: Eduardo Gonzalez
Other Author's Institution: Biomedical Engineering Department, Zhejiang University, China. Email:moreira80@gmail.com

Abstract: Obtaining an ECoG signal requires an invasive procedure in which brain activity is recorded from the cortical surface. In contrast, obtaining EEG recordings requires the non-invasive procedure of recording the brain activity from the scalp surface, which allows EEG recordings to be performed more easily on healthy humans. In this work, a technique previously used to study spatial-temporal patterns of brain activity on animal ECoG was adapted for use on EEG. The main issues are centered on solving the problems introduced by the increment on the interelectrode distance and the procedure to detect stable frames. The results showed that spatial patterns of beta and gamma activity can also be extracted from the EEG signal by using stables frames as time markers for feature extraction. This adapted technique makes it possible to take advantage of the cognitive and phenomenological awareness of a normal healthy subject.
Key words: EEG; spatial-temporal pattern, stable phase structure, frames.

INTRODUCTION

Today there is increasing evidence that brain dynamics is self-organizing and scale-free (Freeman 2004a; Freeman 2004b; Freeman 2007a; Freeman 2007c, Fingelkurts and Fingelkurts 2001, Fingelkurts and Fingelkurts 2004, Stam *et al.* 2003). Several different techniques are currently used in order to describe brain activity on different scales: multiple spike activity (MSA) to describe microscopic activity, local field potentials (LFP) and electrocorticograms (ECoG) for mesoscopic activity, and electroencephalograms (EEG) and brain imaging (MEG and fMRI) for macroscopic activity. The action-perception cycle has been defined as the circular sequence from microscopic activity, which is evoked by receptor input from sensation, to macroscopic activity in concept formation and the reverse process dominates in motor cortices (Freeman 2007b; Freeman 2007a; Freeman 2007c). In both cases, there are intermediate integration—differentiation processes on the mesoscopic scale that frequently yield ECoG spatial-temporal patterns with chaotic carrier waves in the beta or gamma range. These patterns are modulations in amplitude (AM) and phase (PM) (Freeman and Van Dijk 1987; Freeman and Barrie 2000; Ohl *et al.* 2000; Freeman and Burke 2003; Freeman *et al.* 2003; Freeman *et al.* 2006b; Freeman *et al.* 2006a).

Spatial-temporal patterns of ECoG signals have been classified with respect to conditioned stimuli (Freeman and Barrie 2000; Freeman 2003; Freeman 2005; Freeman *et al.* 2006b; Freeman *et al.* 2006a, Lehmann *et al.* 1998). These patterns are described as stable frames with carrier frequencies in the beta or gamma bands that recur at similar rates in the theta or alpha bands (Freeman 2006, Fingelkurts and Fingelkurts 2001, Fingelkurts and Fingelkurts 2004). They emerge after sudden jumps in cortical activity called state transition (Freeman 2004a; Freeman 2006). Phase modulation (PM) patterns have a radial symmetry similar to that of a cone. The apex marks the nucleation site of the AM patterns. AM patterns classified with respect to conditioned stimulus have been localized using the pragmatic information index (Freeman 2005; Freeman 2006; Freeman 2007a) and identified with chaotic phase transitions (Kozma and Freeman 2002).

Thus far ECoG recording has been used to study spatial-temporal patterns at the mesoscopic scale of brain electrical activity that is recorded directly from the cortical surface. On the one hand, it is an invasive procedure, and surgery is necessary in order to fix or remove the electrode array to or from the brain cortex. This procedure is commonly used with animals and occasionally with humans who have brain diseases that require surgery or are victims of global paralysis (Hinterberger *et al.* 2003). On the other hand, EEG recording is a procedure in which electrical activity is recorded from the surface of the scalp through metal electrodes (Niedermeyer and Lopes da Silva 2005). This is a completely non-invasive procedure that can be applied repeatedly to patients, normal adults and children with virtually no risk or limitation. Consequently, it is a research interest to adapt the techniques of ECoG to EEG in order to more easily detect and classify spatial-temporal patterns of brain activity.

In this paper, an EEG database that was previously used to study Event Related Potentials (ERP) (Begleiter *et al.* 1995; Zhang *et al.* 1995; Zhang *et al.* 1997) was employed to analyze the EEG from experiments trial by trial and detect spatial amplitude patterns in EEG activity. Subjects had engaged in an object recognition task during the EEG recordings (Zhang *et al.* 1995; Zhang *et al.* 1997). Similar methods previously used to localize and classify AM patterns in ECoG (Barrie *et al.* 1996; Kozma and Freeman 2002; Freeman 2004b; Freeman *et al.* 2006b, Ruiz *et al.* 2007) were applied to EEG. Owing to the well known differences in scale and resolution between ECoG and EEG, adjustments in the technique to identify stable frames and estimated frame gradient were necessary to make this method suitable for use with EEG signals. Stable frames were used as time markers to extract high dimensional feature vectors. A multidimensional scaling technique of nonlinear mapping was applied to produce 2-D visualization and to reduce the dimension of the feature vectors (Sammon 1969; Freeman 2005; Freeman 2006). Classification of these vectors was done using the Back-Propagation (BP) neural network.

Frames obtained from the EEG recording had similar characteristics and parameters as frames obtained from ECoG (Freeman 2004b; Freeman *et al.* 2006b). The mean level of classification for EEG was comparable to that for ECoG, higher than 75%, which shows for the first time that, owing to the scale-free properties of brain activity, these techniques adapted from ECoG can be employed to extract useful information noninvasively from scalp EEG.

DATA SELECTION AND PREPROCESSING

The data used in this work were available from Lester Ingber (Ingber, 1999). The data consist of a set of measurements from 64 electrodes placed on a scalp at standard sites (AEA 1990) as shown in Fig. 1. The sample rate was 256 Hz and the signal duration was 1 second. All scalp electrodes were referred to as Cz. The signals were amplified with a gain of 10,000 by Ep-A2 amplifiers with a band pass between 0.02 and 50 Hz, and recorded on a Concurrent 55/50 computer. Trials with excessive eye and body movements (>73.3 uV) were rejected on-line.

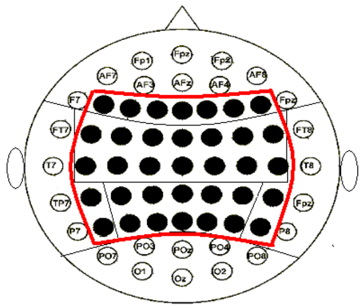

Figure 1: Location of the 64-electrode array. For these experiments, a subset of 35 electrodes was selected (black dots).

A set of figures from the Snodgrass and Vanderwart picture set were chosen as stimuli (Snodgrass and Vanderwart 1980). During the experiments, each subject was exposed to either a single stimulus (S1) to become familiar with the figures, or to two stimuli (S1 and S2) in order to perform a recognition task. The two stimuli were displayed in either a matched condition (S1 was identical to S2) or in a non-matched condition (S1 differed from S2).The subject’s task was to decide whether or not the second picture (S2) was identical to the first stimulus (S1). After the presentation of S2 on each trial, the subjects were asked to press a mouse button in one hand if S2 matched S1 and to press a mouse button in the other hand if S2 differed from S1. All figures selected as stimulus represented a different concrete object and were easily identifiable. The stimuli were presented on a white background at the center of a computer monitor. The picture size ranged from 5~10 cm in high and 5~10 cm in wide, and they were displayed for 300 ms.

The database consists of recordings from two groups: alcoholic subjects and control subjects (with no symptoms of alcoholism or other diseases). In this work, in order to have normal EEG to use for analysis, only recordings from the control subjects were used to carry out the experiments.

Recordings from each control subject were visually inspected to select an appropriate set of recordings for analysis. All subjects with fewer than 20 trials per stimuli or more than 3 noisy channels were rejected; a total of 14 subjects were finally selected. With the aim of avoiding electromyographic noise, an array of 35 electrodes, which mainly consisted of the frontoparietal electrodes, were selected (Fig. 1).

The raw EEG data was visually inspected, and bad channels were replaced by the mean of the adjacent channels. The signals were then demeaned and normalized (Freeman 2005). The temporal power spectral density (PSD) was estimated for each channel and then averaged for each trial and subject. A temporal band pass filter was applied to select the frequency range of interest (Freeman 2004a; Freeman 2004b; Freeman 2005; Freeman 2006) prior to the application of the Hilbert Transform (HT).

AM PATTERNS LOCATION

The Hilbert Transform was used to obtain the analytic amplitude and analytic phase of the EEG signals (Barlow 1993; Freeman 2004a; Freeman 2004b). The analytic phase was used to calculate the parameters of instantaneous frequency and instantaneous gradient. These parameters were used to detect stable frames and estimate the other parameters of frames (Freeman 2004b; Freeman *et al.* 2006b; Freeman *et al.* 2006a). AM patterns were observed during the time samples turned out by stable frames. The feature vectors were selected as the “rms” values of the analytic amplitude within stable frames on the 35 electrodes. The 35 dimensional features were then transformed to a two-dimensional feature vector using Sammon maps (Sammon 1969; Freeman 2005; Freeman 2006).

Detecting stable frames

Cone fitting or spatial-temporal covariance methods to detect frames have been used in the past with similar results (Freeman 2004b; Freeman *et al.* 2006b; Ruiz *et al.* 2007). Thus, using the spatial-temporal covariance method, thresholds for analytic phase covariance (*te1*) and analytic amplitude covariance (*te2*) were set. A time sample phase was selected as a frame candidate only if the analytic phase covariance was lower than *te1*, the analytic amplitude covariance was higher than *te2*, the sign of the instantaneous gradient did not change from one sample to next, and the instantaneous frequency was within the temporal band used.

Between the time points that frame candidates were detected, frame frequency and gradient were calculated by Eq 1 & 2:

$$F_N = \frac{1}{n}\sum^{n} \mathrm{w}_i(t_n) \qquad (1)$$

$$\gamma_N = \frac{1}{n}\sum^{n} \gamma(t_n) \qquad (2)$$

where n was the number of time steps across which a stable frame had been defined, wi was the instantaneous frequency and γ was the instantaneous gradient. Other parameters, such as frame phase velocity and frame diameter (see Eq 3 & 4), were derived from these equations (Freeman 2004b; Freeman *et al.* 2006b). The frame rate was defined as the inverse of the time lapse between successive starting points of stable frames, and the duration was given by the number of digitizing over which the stable frame was detected.

$$B = \frac{2\pi\, \mathrm{F}_N}{1000|\gamma_N|} \qquad (3)$$

$$D_x = \frac{\pi}{2}\frac{1}{|\gamma_N|} \qquad (4)$$

After that, supplemental anatomical and physiological evaluations were made of the acceptable parameter rank in order to exclude spurious frames from the analysis. The phase velocity had to be within the range of conduction velocities of cortical axons (1-10 m/s), frame duration should have been more than 15 ms on the beta band or 10 ms on the gamma band, and frame diameter had to be smaller than the width of the cerebrum, 200 mm (Freeman 2004b; Freeman *et al.* 2006b).

Estimating instantaneous frequency and gradient

Instantaneous frequency, or the rate of change in phase with time (Hz), was estimated as the successive differences of the unwrapped analytic phase divided by the digitizing step (Freeman 2004b; Freeman *et al.* 2006a; Freeman *et al.* 2006b). This parameter is not interelectrode distance dependent.

On the other hand, instantaneous gradient, the rate of change in phase with distance (rad/mm), is interelectrode distance dependent. The interelectrode distance in previous work was in the order of 3 mm (Barrie, Freeman *et al.* 1996; Freeman *et al.* 2006a; Freeman *et al.* 2006b). For EEG, the interelectrode distance was increased to the order of 3 cm (Zhang *et al.* 1995), but the analytic phase values are between –pi and pi in both cases (Barlow 1993). The analytic phase differences are lower than 2pi radian regardless of whether the interelectrode distance measures in millimeters, centimeters, or meters. Also, within the time period that the stable frames shows up, the phase should be smooth and with little change from one electrode to another and from one time sample to the next, which produces very low analytic phase differences.

For EcoG, cone fitting was normally used to estimate the instantaneous gradient (Freeman and Barrie 2000; Freeman and Rogers 2003; Freeman 2004b; Freeman *et al.* 2006a; Freeman *et al.* 2006b), but it is a highly time-consuming method and has technical constraints that make it difficult to apply to EEG signals (Freeman 2004b; Freeman *et al.* 2006a). In (Ruiz *et al.* 2007), a new method to estimate the instantaneous gradient was presented. In this method, the instantaneous gradient was estimated as the slope (m) of the line fitted to the differences between every analytic phase value and the other phase values for each interelectrode distance (see Fig. 2a). The results obtained were similar to the results produced by the cone fitting method (Ruiz *et al.* 2007).

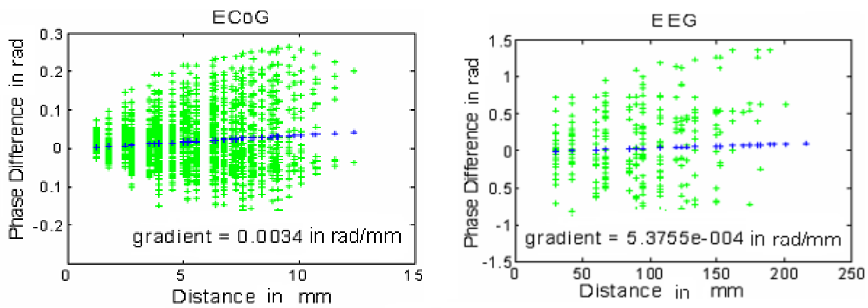

(a) **(b)**

Figure 2: Gradients (rad/mm) were estimated as the slope of the line (blue/dark) fitted to the difference between every analytic phase value and the other phase values for each interelectrode distance (green/light): a) 64 channels of ECoG, and b) 35 channels of EEG. Due to the increase of interelectrode distance, the gradient of the EEG signal was very low, which caused frame velocity to be out of the range of conduction velocity for the cortex. This example is from a signal filtered on the beta range, 12-30 Hz.

The slope of one line is the relation between the variation in the Y axis (phase difference) and X axis (interelectrode distance) for two points. Due to the increase of interelectrode distance, the gradient values for EEG were drastically reduced, even though the phase differences between electrodes had increased (see Fig. 2). Gradient values estimated by this method induced frame velocities higher than 150 m/s, and after physiological criterion for frame detection were applied (Freeman 2004b; Freeman *et al.* 2006b; Freeman *et al.* 2006a), no stable frames were detected. For that reason, some changes in the gradient estimation method were made. The global instantaneous gradient was estimated as the slope of the line between the points of minima and maxima phase for each time sample (see Fig. 3). Using this method to estimate the gradient frame velocity was within the range of conduction velocity for the cortex, 10 m/s.

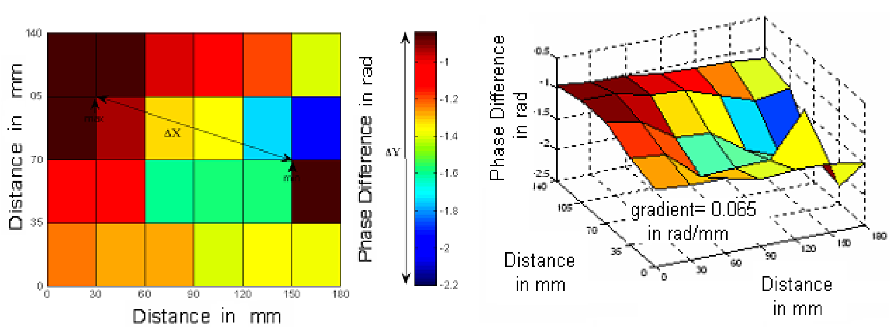

Figure 3: A global gradient (rad/mm) index was estimated for EEG signals as the slope of the line between the points of minima and maxima phase for each time sample. This example is from a signal filtered on the beta range, 12-30 Hz.

CLASSIFICATION PROCESS

Two classes were defined to carry out the classification process. Single stimulus presentation was defined as class1 and two stimuli presentation as class2. Class2 presentations can be in a matched condition (first stimulus identical to second stimulus) or in a non-matched condition (first stimulus different from second stimulus).

The Sammon map iteratively mapped the location of points defined from a high-dimensional space (here 35) to low-dimensional space (here 2), preserving the relative distances between points (Sammon 1969; Freeman 2005; Freeman 2006). After mapping, the feature vectors were labeled for graphic display and classification. BP networks were used to perform the classification.

Two-layer BP networks were used on linearly separable problems. Alternatively, if the problem required a boundary region other than a line, a three-layer BP was used to define it (Duda *et al.* 2000; MATLAB®). Two-layer BP and three-layer BP were used for classification (see Fig. 4). The training set consisted of 6 trials per class, and the test set conformed in all trials. The number of neurons on the hidden layer varied from 3 to 7, and the best performance was achieved with 5 neurons.

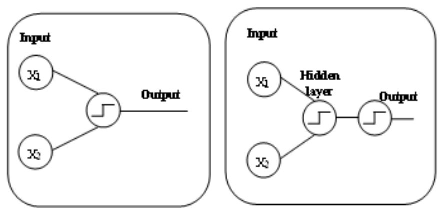

Figure 4: Two-layer and three-layer BP networks were used in classification. The first was used on linearly separable problems and the second on non-linearly separable problems.

RESULTS

The EEG signals were band pass filtered between 0.02 Hz and 50 Hz during the recording process, and for that reason, only the frequencies between 4 to 50 Hz were analyzed. Figure 5 shows an example of PSD displayed in log-log coordinates. PSD revealed a $1/f^{\alpha}$ form with upward deviations from a straight line in the frequency range from 10 to 45 Hz, and α varied from -1 to -3 (Freeman 2004a; Freeman *et al.* 2006b).

Frequencies from 12 Hz to 30 Hz (beta band) and 30 Hz to 45 Hz (low gamma) were used as the temporal band filter settings. Stable frame parameters were estimated for each subject and each class on the beta and gamma bands.

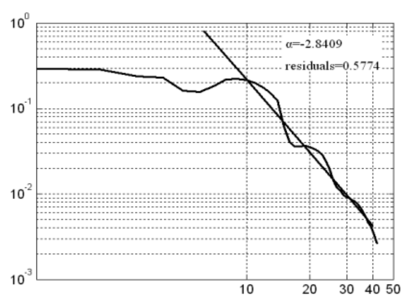

Figure 5: PSD revealed a $1/f^{\alpha}$ form with upward deviations in the beta and gamma range, α varied from -1 to -3.

Figure 6 shows the mean frame parameter value of each subject. Frequency, velocity and duration are clearly distinguishable from frames on the beta or gamma bands. Gradient, diameter and rate values overlap for some subjects. In general, stable frames from the beta band have lower carrier frequencies, velocities, diameters, rates, and a longer duration than stable frames on the gamma band. The differences of stable frame parameters between classes were not obvious.

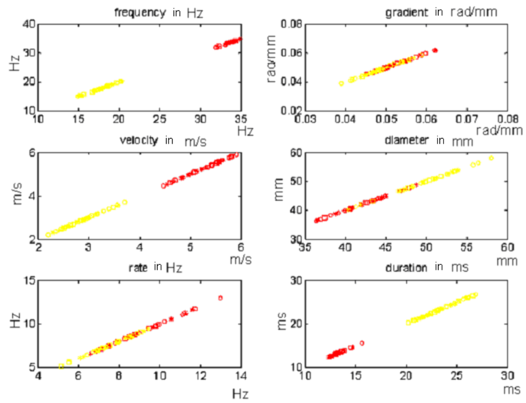

Figure 6: Stable frame parameters on beta (yellow/light) and gamma (red/dark) bands for each class: * class1, o class2 matched condition, □, class2 non-matched condition. Stable frame parameters for each band are clearly distinguishable, but no differences in frame parameters were observed within the classes on the same band.

Feature vectors were extracted as the “rms” values of analytic amplitude on each electrode within the time periods where stable frames were detected. Sammon maps were used to visualize the distribution of the features (see Fig. 7) and to transform the 35 dimensional feature vectors into a two dimensional feature vectors. Comparable maps were obtained from the beta and gamma bands, so only a few maps from the beta band are presented here.

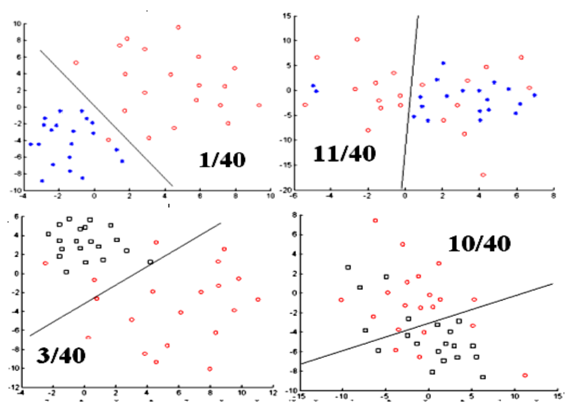

(a) **(b)**

Figure 7: Sammon maps allow for the visualization of the feature vectors in two-dimensional space. a) subject c344 b) subject co2c347. Top: class1 (red “o”) vs class2 matched condition (blue “*”), bottom: class1 (red “o”) vs class2 non-matched condition (black “□”), on beta band. A line was drawn to separate clusters and features positioned on the wrong side of the line calculated.

Clusters of vectors were distinctly formed for almost all subjects. A line was drawn in the display plane between the clusters on the premise of linear separability, showing that for some subjects the line almost separates the classes but not for others. Because of this, a three-layer BP was used for classification as well. Figure 8 shows the Correct Classification rate (CC) in percent per subject for a two layer and a three layer BP network.

The correct classification rate of beta and gamma patterns was around 70% using a two-layer BP network for almost all subjects and around 80% using a three-layer BP network. The three-layer BP network improved the mean classification rate about 5% because for some subjects the clusters were well defined and the best boundary region was a line.

Correct classification rates that were higher than 62.5 % for all subjects show that spatial patterns of beta and gamma activity can be extracted from the EEG signal. Differences between subjects can be ascribed to subjects' previous experiences, level of attentiveness, and level of expectation prior to the presentation of the stimulus (Freeman 2004a; Freeman 2005; Freeman 2006).

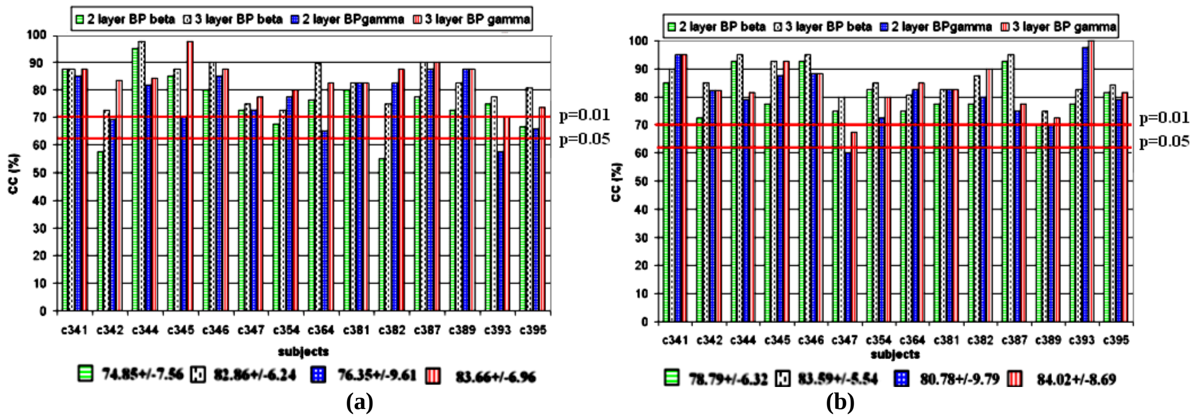

Figure 8: Classification rate a) class1 and class2 matched condition b) class1 and class2 non-matched condition, at the bottom the mean +/- standard error of classification across all subjects. The 3 layer BP network improved the mean classification rate by around 5 percent.

CONCLUSIONS

Phase transitions that preceded the emergence of AM and PM modulation patterns were detected using the covariance method (Ruiz *et al.* 2007). The global gradient estimation was used to detect stable frames and these stable frames were used as time marker for feature extraction.

The hyperspace feature vectors were mapped into 2-space in order to display clusters of points that represent the differing spatial patterns corresponding to both the single stimulus presentation and the double stimuli presentation. The 2-space feature vectors were used for classification of these patterns.

Similar CC% values were obtained for patterns on the beta and gamma bands. The CC% was higher than 62.5 % for all subjects (p=0.05 for binary classification), which shows that spatial patterns of beta and gamma activity can also be extracted from the EEG signal using this adapted technique.

This adapted technique can provide the foundation needed to investigate the cerebral dynamics of learning. Furthermore, it also allows researchers to take advantage of the cognitive and phenomenological awareness of a normal healthy subject and their verbal description of mental states by using a non-invasive technique to record the brain's electrical activity.

Previous studies have shown that phase transitions are different according to the temporal band pass selected. Future studies of frequency bands and bandwidth carrying levels of meaningful information should be done.

Acknowledgements

This research is supported by the National Creative Research Groups Science Foundation of China (NCRGSFC: 60421002), the Natural Science Foundation of China (Grant No. 60874098) and the National High Technology Research and Development Program of China (863 Program 2007AA042103). The human data was collected by Henri Begleiter and associates at the Neurodynamics Laboratory at the State University of New York Health Center at Brooklyn and prepared by David Chorlian.

References

American Electroencephalographic Association. (1990) Standard Electrode Position Nomenclature.
Barlow, J. S., 1993. The electroencephalogram: its patterns and origins. Cambridge, Mass, MIT Press.

Barrie, J. M., Freeman, W. J. and Lenhart, M. D,. (1996). "Spatiotemporal analysis of prepyriform, visual, auditory, and somesthetic surface EEGs in trained rabbits." *Journal of Neurophysiology* 76(1): 520-539.

Begleiter, H., Porjesz, B. and Wang, W., 1995. “Event-related brain potentials differentiate priming and recognition to familiar and unfamiliar faces” *Electroencephalography and Clinical Neurophysiology* 94(1): 41-49. [doi:10.1016/0013-4694(94)00240-L]

Duda, R. O., Hart, P. E. and Stork, D. G., 2000. Pattern Classification. New York, Wiley. [doi:10.1007/s00357-007-0015-9]

Fingelkurts A .A., Fingelkurts A. A., 2001. “Operational architectonics of the human brain biopotential field: Towards solving the mind-brain problem”. *Brain & Mind*, 2:261-296. [doi: 10.1023/A:1014427822738]

Fingelkurts A .A., Fingelkurts A. A., 2004. “Making complexity simpler: Multivariability and metastability in the brain”. *Int J.Neurosci*, 114:843-862. [doi: 10.1080/00207450490450046]

Freeman, W., 2007a. "Definitions of state variables and state space for brain–computer interface. Part 2. Extraction and classification of features vectors" *Cognitive Neurodynamics* 1(2): 85-96. [doi:10.1007/s11571-006-9002-9]

Freeman, W., 2007b. Proposed Cortical “Shutter” Mechanism in Cinematographic Perception. Neurodynamics of Cognition and Consciousness: 11-38. [doi:10.1007/978-3-540-73267-9]

Freeman, W. J., 2003. "A Neurobiological Theory of Meaning in Perception Part II: Spatial Patterns of Phase in Gamma EEGs from Primary Sensory Cortices Reveal the Dynamics of Mesoscopic Wave Packets." *International Journal of Bifurcation and Chaos* 13(9): 2513-2535. [doi:10.1142/S0218127403008156]

Freeman, W. J., 2004a. "Origin, structure, and role of background EEG activity. Part 1. Analytic amplitude." *Clinical Neurophysiology* 115(9): 2077-2088. [doi:10.1016/j.clinph.2004.02.029]

Freeman, W. J., 2004b. "Origin, structure, and role of background EEG activity. Part 2. Analytic phase." *Clinical Neurophysiology* 115(9): 2089-2107. [doi:10.1016/j.clinph.2004.02.028]

Freeman, W. J., 2005. "Origin, structure, and role of background EEG activity. Part 3. Neural frame classification." *Clinical Neurophysiology* 116(5): 1118-1129. [doi:10.1016/j.clinph.2004.12.023]

Freeman, W. J., 2006. "A cinematographic hypothesis of cortical dynamics in perception." International *Journal of Psychophysiology* 60(2): 149-161. [doi:10.1016/j.ijpsycho.2005.12.009]

Freeman, W. J., 2007c. "Definitions of state variables and state space for brain-computer interface. Part 1. Multiple hierarchical levels of brain function" *Cognitive Neurodynamics* 1(1): 3-14. [doi 10.1007/s11571-006-9001-x]

Freeman, W. J. and Barrie, J. M., 2000. "Analysis of spatial patterns of phase in neocortical gamma EEGs in rabbit." *Journal of Neurophysiology* 84(3): 1266–78.

Freeman, W. J. and Burke, B. C., 2003. "A Neurobiological Theory of Meaning in Perception Part IV: Multicortical patterns of amplitude modulation in gamma EEG." *International Journal of Bifurcation and Chaos* 13(10): 2857-2866. DOI: 10.1142/S0218127403008302

Freeman, W. J., Burke, B. C. and Holmes, M. D., 2003. "Aperiodic phase re-setting in scalp EEG of beta-gamma oscillations by state transitions at alpha-theta rates." *Human Brain Mapping* 19(4): 248-272. [doi: 10.1002/hbm.10120]

Freeman, W. J., Holmes, M. D., West, G. A. and Vanhatalo, S., 2006a. "Dynamics of human neocortex that optimizes its stability and flexibility." *International Journal of Intelligent Systems* 21(9): 881-901. [doi:10.1002/int.v21:9]

Freeman, W. J., Holmes, M. D., West, G. A. and Vanhatalo, S., 2006b. "Fine spatiotemporal structure of phase in human intracranial EEG." *Clinical Neurophysiology* 117(6): 1228-1243. [doi:10.1016/j.clinph.2006.03.012]

Freeman, W. J. and Rogers, L. J., 2003. "A Neurobiological Theory of Meaning in Perception Part V: Multicortical patterns of phase modulation in gamma EEG." *International Journal of Bifurcation and Chaos* 13(10): 2867-2887. [doi:10.1142/S0218127403008296]

Freeman, W. J. and Van Dijk, B. W., 1987. "Spatial patterns of visual cortical fast EEG during conditioned reflex in a rhesus monkey." *Brain Research Reviews* 422(2): 267-276. [doi:10.1016/0006-8993(87)90933-4]

Hinterberger, T., Kübler, A., Kaiser, J., Neumann, N. and Birbaumer, N., 2003. "A brain-computer interface (BCI) for the locked-in: comparison of different EEG classifications for the thought translation device." *Clinical Neurophysiology* 114(3): 416-425. [doi:10.1016/S1388-2457(02)00411-X]

Ingber, L. (1999) EEG database. from http://kdd.ics.uci.edu/databases/eeg/eeg.html

Kozma, R. and Freeman, W. J., 2002. "Classification of EEG patterns using nonlinear dynamics and identifying chaotic phase transitions." *Neurocomputing* 44: 1107-1112. [doi:10.1016/S0925-2312(02)00429-0]

Lehmann, D., Strik, W.K., Henggeler, B., Koenig, T. and Koukkou, M., 1998. "Brain electric microstates and momentary conscious mind states as building blocks of spontaneous thinking: I. Visual imagery and abstract thoughts". *Int. J. Psychophysiol*. 29: 1-11. [doi: 10.1016/S0167-8760(97)00098-6]

MATLAB®., 2007. User Guide, R2007b http://www.mathworks.com.

Niedermeyer, E. and Lopes da Silva, F., 2005. Electroencephalography: Basic principles, clinical applications and related fields. Baltimore, Lippincott Williams & Wilkins.

Ohl, F. W., Schulze, H., Scheich, H. and Freeman, W. J., 2000. "Spatial representation of frequency-modulated tones in gerbil auditory cortex revealed by epidural electrocorticography." *Journal of Physiology-Paris* 94(5-6): 549-554. [doi:10.1016/S0928-4257(00)01091-3]

Ruiz, Y., Li, G.., Freeman, W. J. and Moreira, E. G., 2007. A New Approach to Detect Stable Phase Structure in High Density EEG Signals The 1st International Conference on Cognitive Neurodynamics ICCN 2007, Shanghai, P.R. China, Springer. DOI: 10.1007/978-1-4020-8387-7

Sammon, J. W., 1969. "A Nonlinear Mapping for Data Structure Analysis." *IEEE Trans. Comput*. 18(5): 401-409. [doi:10.1109/T-C.1969.222678]

Snodgrass, J. G. and Vanderwart, M., 1980. "A standardized set of 260 pictures: Norms for name agreement, image agreement, familiarity, and visual complexity." *Journal of Experimental Psychology: Human Learning and Memory* 6(2): 174-215. [doi:10.1037/0278-7393.6.2.174]

Stam C. J., Breakspear M, Cappellen A. Dijk B. W., 2003. "Nonlinear synchronization in EEG and whole-head MEG recordings of healthy subjects". *Hum Brain Mapp* 19:63-78. [doi: 10.1002/hbm.10106]

Zhang, X. L., Begleiter, H., Porjesz, B. and Litke, A., 1997. "Visual object priming differs from visual word priming: an ERP study." *Electroencephalography and Clinical Neurophysiology* 102(3): 200-215. [doi:10.1016/S0013-4694(96)95172-3]

Zhang, X. L., Begleiter, H., Porjesz, B., Wang, W. and Litke, A., 1995. "Event related potentials during object recognition tasks." *Brain Research Bulletin* 38(6): 531-538. [doi:10.1016/0361-9230(95)02023-5]